Process Safety and Environmental Protection 147 (2021) 300–310

Contents lists available at ScienceDirect

Process Safety and Environmental Protection

journal homepage: www.elsevier.com/locate/psep

Modeling the corrosion rate of carbon steel in carbonated mixtures of MDEA-based solutions using artificial neural network

Qiang Li[a,b], Dongxu Wang[a], Mingyu Zhao[a], Minghao Yang[a], Jianfeng Tang[a,b,*], Kai Zhou[c]

[a] College of Pipeline and Civil Engineering, China University of Petroleum (East China), Qingdao, Shandong, 266580, China
[b] Shandong Key Laboratory of Oil & Gas Storage and Transportation Safety, China
[c] Shandong Special Equipment Inspection Institute Co., Ltd., Jinan, Shandong, 250101, China

ARTICLE INFO

Article history:
Received 2 April 2020
Received in revised form 20 August 2020
Accepted 23 August 2020
Available online 22 September 2020

Keywords:
Amine solution
Corrosion prediction
ANN
Carbon steel

ABSTRACT

Amine-based CO_2 absorption process has the benefit of purifying produced natural gas and reducing greenhouse gas emissions; however, it is associated with corrosion issues. This work aims to develop a corrosion prediction model for carbon steel in methyldiethanolamine (MDEA)-based binary mixtures with monoethanolamine (MEA), diethanolamine (DEA), or piperazine (PZ) at various concentrations using artificial neural network (ANN). Experimental studies of Q345R steel are performed, and corrosion rate data obtained by weight loss method is used to create a database for training and testing of the ANN model. A backpropagation (BP) multilayer perceptron (MLP) network with three layers is proposed. The number of input variables for the input layer is optimized after performing a correlation analysis. Effect of neuron quantity in the hidden layer on ANN model performance is studied; increasing the neuron quantity in the hidden layer is found to enhance the training accuracy and reduce the testing accuracy. A new index, max absolute relative deviation (MARD), is introduced to quantify the performance of the ANN model. The developed 5-8-1 type ANN model is able to give a MARD of 8.66 %. The same corrosion rate database is used to develop the SVM model, in which radial basis function (RBF) is used as the kernel function, and K-fold cross-validation technique is applied to select the optimal model values. A comparison of performance in both training and testing shows that the ANN model outperforms the SVM model.

1. Introduction

Aqueous amine solutions have been widely used in the gas industry to absorb acid gasses, including CO_2 and H_2S. In the production of natural gas, such acidic gases not only degrade the gas quality but also pose operational difficulties for the downstream processes (Rennie, 2006; Nainar and Veawab, 2009; Saghafi and Arabloo, 2017). In addition, CO_2 absorption with amine solutions also has the benefit of reducing greenhouse gas emissions; therefore, it plays a vital role in the carbon capture and storage (CCS) processes (Zheng et al., 2014; Gunasekaran, 2012). However, the amine-based CO_2 absorption process is associated with corrosion issues (Yu et al., 2016; Emori et al., 2017). Besides the corrosion caused by solution of dissolved of CO_2 in water, amine solutions have also been found to cause corrosion to pipings and equipment (Veawab et al., 1999). Especially after multiple cycling applications in the high-pressure and high-temperature conditions, heat stable salts (HSS) could form due to amine solution degradation (Nainar and Veawab, 2009), creating a more corrosive environment.

Over the years, amines mixtures are preferred as compared to a single amine in CO_2 absorption process. The amine mixtures can combine the advantages of high CO_2 reaction rate of the primary (MEA) or secondary amines (DEA) with the low heat of reaction of the tertiary amines (MDEA) (Gunasekaran, 2012), thus offering high absorption capacity with high energy efficiency (Eustaquio-Rincón et al., 2008). In addition, high resistance to degradation and low corrosivity could also be achieved (Labiyi, 2016).

There are differences in corrosivity for all the single amine solutions and mixtures that are used in CO_2 absorption processes. Also, the corrosivity of the mixtures could vary due to different concentration ratios. With so many amine solution options, it is preferred to have a model that can predict the corrosion rate of carbon steels for various amine types and concentrations. Choi et al. (2012) developed a predictive mechanistic model for carbon steel corrosion in CO_2-loaded MDEA systems by considering the thermodynamic

* Corresponding author at: No. 66 Changjiang West Road, Huangdao District, Qingdao, Shandong, 266580, China.
E-mail address: tangpaper@126.com (J. Tang).

https://doi.org/10.1016/j.psep.2020.08.035
0957-5820/

equilibria and electrochemical reactions, and this model was validated to be applicable for the uniform corrosion prediction in MDEA-CO_2-H_2O system (Choi et al., 2012). Labiyi (2016) developed a mechanistic model for the prediction of iron corrosion in MEA-CO_2-H_2O system, and the model was shown to be able to clarify the impact of operating parameters on corrosion rates (Labiyi, 2016). These prediction models have strong theoretical background and were proved to have a good prediction ability for a specific amine-solution system under specific conditions. However, their application to other amine solutions, especially amine mixtures and those solutions where HSS may form, is questionable. Corrosion in amine solutions is involved with multiple influencing factors, and it could be challenging, if not impossible, to develop such a mechanistic model that applies to multiple amine solution conditions. To solve this problem, a model based on ANN emerges as an alternative solution.

The design of the ANN approach is based on the nervous system of the human brain, and it was widely used due to its excellent robustness and abilities in solving non-linear and multivariable problems associated with complex physio-chemical processes (Ghiasi et al., 2014; Rocabruno-Valdés et al., 2019). Essentially, ANN has been successfully used in corrosion predictions, in addition to its application in various other disciplines (Abiodun et al., 2018). At the same time, various factors are used to assess the performance of the ANNs. Xu and Jin (2018) applied ANN models to link non-destructive parameters and predicted the rebar corrosion levels in concrete prisms. The BP type ANN model is shown to give predictions with a relative error as small as 1.32 %, and the maximum relative error is 30.85 % (Xu and Jin, 2018). Rocabruno-Valdés et al. (2019) developed a direct ANN to predict corrosion rates of metals in different biodiesel. In this work, the simulated data with the BP ANN model were compared with the experimental result through the linear regression model with a correlation coefficient of 0.9885 and a mean square error (MSE) of 2.15×10^{-4} (Rocabruno-Valdés et al., 2019). Colorado-Garrido et al. (2008) extend the application of ANN in predicting electrochemical impedance Nyquist plots during corrosion inhibition of a pipeline, a coefficient of 0.984/0.996 shows the good-quality prediction of the ANN model (Colorado-Garrido et al., 2008). Hu et al. (2019) employed the BP type ANN model to predict polarization curves, which were commonly used as the basic method to explain the corrosion kinetic behavior, under different complex sea environments. In this work, the coefficient of determination, R^2, was used to assess the accuracy of fitting, and R^2 in both training and testing was found to be larger than 0.92 (Hu et al., 2019). Recently, Saghafi and Arabloo (2017) used the ANN algorithm to model CO_2 solubility in MEA, DEA, TEA, and MDEA aqueous solutions as a function of CO_2 partial pressure, temperature, and concentration of amine solutions. Besides R^2, root mean square square (RMSE), average relative deviation (ARD), and average absolute relative deviation (AARD) were utilized to quantify the errors in modeling process (Saghafi and Arabloo, 2017). Until now, efforts to develop an ANN model that is able to characterize the corrosion rate of carbon steel in various amine solutions has rarely been seen in the literature. This paper, therefore, fills this gap by studying the essential details for the development of an accurate and reliable ANN model for corrosion in amine solutions.

It is recognised that a systematic and large-in-number database is crucial for the development of a reliable and accurate ANN based prediction model. A review of current openly available experimental data in the literature on studies relating to corrosion in amines solutions shows that the types of amine solutions and the environmental conditions varied considerably (Gunasekaran, 2012; Labiyi, 2016; Gunasekaran et al., 2013; Tanthapanichakoon and Veawab, 2005; Campbell et al., 2016). More so, the corrosion rates were determined using different methods. In this study, however, experiments were designed and performed in such a way to create a systematic and complete database for an ANN model development. Corrosion of carbon steel Q345R was studied in binary amine mixtures of MDEA with MEA, DEA, or PZ at different concentrations. Weight loss method was used to obtain the corrosion rate, the solution pH and conductivity were also measured.

2. Experimental

2.1. Specimen preparation

The specimens used in the experimental studies were made of Q345R steel, of chemical composition (by mass fraction, %) of C 0.14, Si 0.41, Mn 1.38, P 0.017, S 0.005, and Fe balance. Each specimen was machined into a plate of dimensions of 50 mm × 25 mm × 2 mm. A hole of 2 mm in diameter was drilled on each specimen for the purpose of hanging during the tests.

Before all tests, the exposed surfaces of the specimens were wet ground with silicon carbide papers sequentially up to 600 grit, cleaned with deionized water and methanol, and dried with a blower. The specimens were then kept in a desiccator before being used.

2.2. Solution preparation and analysis

Binary amine mixtures of MDEA with DEA, MEA, or PZ at different concentrations were prepared from analytic reagent chemicals and deionized water. MDEA was used as the base solution, while DEA, MEA, or PZ were used as the additives.

Noting that the constituent of amine solutions has an influence on many aspects, including absorption capacity, absorption rate (Chen et al., 2014), time taken for regeneration, regeneration heat efficiency, foaming characteristics (Zhang, 2017) and corrosion rate of carbon steels, in gas absorption processes, concentrations of the amine solutions were carefully selected. A recommended guideline for maximum amine concentration to control the corrosion rate is available as: 10∼20 wt% for MEA, 20∼40 wt% for DEA, 50∼55 wt% for MDEA (Nielsen et al., 1995). Accordingly, the constituent percentage of the binary amine solutions was decided, as shown in Appendix.

HSSs have been a growing concern in amine solutions. The presence of HSS is believed to decrease the acid gas absorption capacity, increase the solution viscosity, increase the solution foaming tendency, increase the solution conductivity, and create a more corrosive environment (Nainar and Veawab, 2009; Tanthapanichakoon and Veawab, 2005; Veldman, 2000). Generally, acids react with the amine by the proton transfer reaction to form HSS (Veldman, 2000):

$$RNH_2 + HA \leftrightarrow RNH_3^+A^- \quad (1)$$

where HA is the acid form of the heat stable salt anion, and A^- is the heat stable salt anion. The corrosion mechanism in the presence of HSS is still under debate (Labiyi, 2016) and need further clarification. Common HSSs found in the CO_2 absorption process are formate, acetate, oxalate, glycolate, malonate, sulfate, sulfite, and so on (Tanthapanichakoon and Veawab, 2005). Among all the HSSs, acetate was found to be more corrosive salt than formate and oxalate (Nainar and Veawab, 2009), and it was also identified as the dominating composition in a typical amine sample that was recovered from the field (Fang, 2004). To include the effect HSS on corrosion rate, a certain amount of acetic aicd was added to the amine mixtures to simulate heat-stable salts formed due to complex degradation and reactions after being circulated in the acid-picking system with amine solutions.

The solutions were prepared as follows: 1) MDEA and additives were weighted according to their required concentrations; 2) MDEA and additives were blended with deionized water to form

a solution of 110 g in weight, and a glass rod was used to stir the solution to get a well-mixed solution. As PZ occurs as a solid at atmosphere temperature, its blended solution was obtained by continuous stirring until it had totally dissolved. 3) Acetic acid was then added. For a lean solution, the weight of added acetic acid was 0.33 g, while for a rich solution, it was 1.1 g. CO_2 was purged into the solution to simulate the rich solution, and the purging process was maintained throughout the test. CO_2 loadings in the rich amine solutions studied are between 0.27 mol/mol amine and 0.36 mol/mol amine. For the lean solution, the purging gas was N_2. CO_2 loading in the lean solution is 0. After the solution was cooled to the atmosphere temperature, the solution pH and conductivity were measured. A pH meter (METTLER TOLEDO) with a precision of 0.01 was used to measure the solution pH. The solution conductivity was measured using a conductivity meter (Shanghai Yueping DDS-11A), which had a precision of 0.001 μs/cm.

Before the temperature was determined, a series of preliminary experiment was performed for both the lean and rich amine solutions. It was found that for both amine solutions, a high increase rate in corrosion was found when the temperature increased from 40 to 80 °C, and a quite small increase rate for temperature between 80 ~ 110 °C (The experimental result is attached in the supplementary data). As a result, a temperature of 80 °C, which was commonly used in the open literature (Veawab et al., 1999; Gunasekaran et al., 2013), was selected for tests in lean solutions and rich solutions. The solution was heated to the designed temperature with a water bath (METTLER TOLEDO), and the temperature was controlled at 80 ± 0.1 °C.

2.3. Experimental setup

During the weight loss test, a precision electric balance (OHAUS CP114) with an accuracy of 0.1 mg was used to measure the weight loss of the specimens. After exposing the prepared solutions for 168 h, the weight loss specimens were collected. They were first cleaned using a scrubbing brush, and then put in a boiled chemical cleaning solution, which contained 20 % NaOH and 200 g/L Zinc powder, for 5 min (G1-03, 2011). The specimens were then further cleaned with deionized water and methanol, dried with a blower, and kept in a desiccator for 24 h before being measured with the precision electric balance.

3. Computational methodology

3.1. Experimental database

Experimental results, i.e., corrosion rate, obtained by weight loss method for various amine compositions and concentrations, were used to create the database for the ANN model development and to validate the model prediction result. A total of 114 groups of experimental data were obtained, as shown in the Appendix. Approximately 10 % of total data, i.e., 12 groups (which were No. 3, 20, 25, 36, 49, 54, 65, 70, 79, 91, 94, and 114 of those listed in Appendix A), was picked out by a random algorithm embedded in MATLAB 2016b and used to test the accuracy of the ANN model. Realizing that there were apparent differences in corrosion rates for the different amine solution types, i.e., lean and rich solutions, six groups of data were selected from each solution type. The remaining 102 groups of data were then used for the ANN model training.

3.2. Correlation analysis

In this study, the experimental conditions, including concentrations of MDEA, DEA, MEA, PZ, pH, and conductivity of the binary mixtures and solution type, were the independent variables while the corrosion rate was the dependent variable. The variable temperature was excluded from the independent variables as the temperature was kept constant for all experimental conditions. The solution type, i.e., lean solution and rich solution, was converted to a virtual variable before it was used as an independent variable. The lean solution was assigned the number of 0, while the rich solution was assigned the number 1.

To identify the variables that are strongly correlated with the corrosion rates, the Pearson's correlation coefficient r, which is a measure of the linear association of two variables, was determined with Eq. (2) as follows (Ahlgren et al., 2003):

$$r = \frac{\sum(x-\bar{x})(y-\bar{y})}{\sqrt{\sum(x-\bar{x})^2 \sum(y-\bar{y})^2}} \quad (2)$$

where x and y are the sample data of two variables, $\bar{x}$ and $\bar{y}$ denotes the means of x and y, respectively. The value of r is between 1 and -1; a positive number indicates a positive correlation, while a negative number indicates a negative correlation. A large absolute value of r means a strong correlation exists between two variables.

3.3. ANN model development

Amongst the many types of ANNs available in the literature (Saghafi and Arabloo, 2017; Abiodun et al., 2018), the MLP was proposed to be the most practical method used in petroleum and natural gas scenarios (Ghiasi et al., 2014). A three-layer MLP, which includes one input layer, one output layer and one hidden layer, was used, as shown in Fig. 1.

Each layer in an ANN has one or more neurons as the fundamental construction blocks. For the input and output layer, the number of neurons equals to the number of inputs and outputs, respectively. There was only one output variable in the output layer, i.e., the corrosion rate, thus the output layer has one neuron. For the input layer, the number of inputs was determined according to the correlation analysis and model prediction result. To determine of the number of neurons in the hidden layer, the empirical equation $h = \sqrt{M+N} + \sigma$ was used (Li et al., 2005). Where M is the number of neurons in the input layer; N is the number of neurons in the output layer; σ is a constant between 1 and 10. Moreover, the effect of number of neurons in the hidden layer was also studied to obtain an optimized neuron quantity in the hidden layer that could contribute to a good ANN model performance.

BP method, a supervised learning technique in ANN (Hu et al., 2019), was used to teach the ANNs how to perform a given task and fit a model to the obtained experimental data using MATLAB 2016b Neural Network Toolbox (Beale et al., 2016b). A performance comparison between multiple training algorithms, including the Levenberg-Marquardt BP algorithm, Bayesian regularization BP algorithm, Scaled conjugate gradient BP algorithm, and Resilient BP algorithm, embedded in MATLAB 2016b, was done. After this, the Levenberg-Marquardt BP algorithm was finally chosen for its lower training time, and its smaller best mean squared normalized error (mean square error (MSE) is defined as the mean of the squares of the difference between the calculated value and the actual value), as also illustrated elsewhere (Rocabruno-Valdés et al., 2019). In addition, the hyperbolic tangent sigmoidal transfer function was used in the hidden layer, while the linear transfer function was applied in the output layer.

3.4. SVM model development

SVMs were also used in developing corrosion prediction models in recent years (Chou et al., 2017; El Amine Ben Seghier et al., 2020). SVM is a supervised machine learning algorithm, its basic principle in the application of prediction is to find a function $f(x)$ that has the

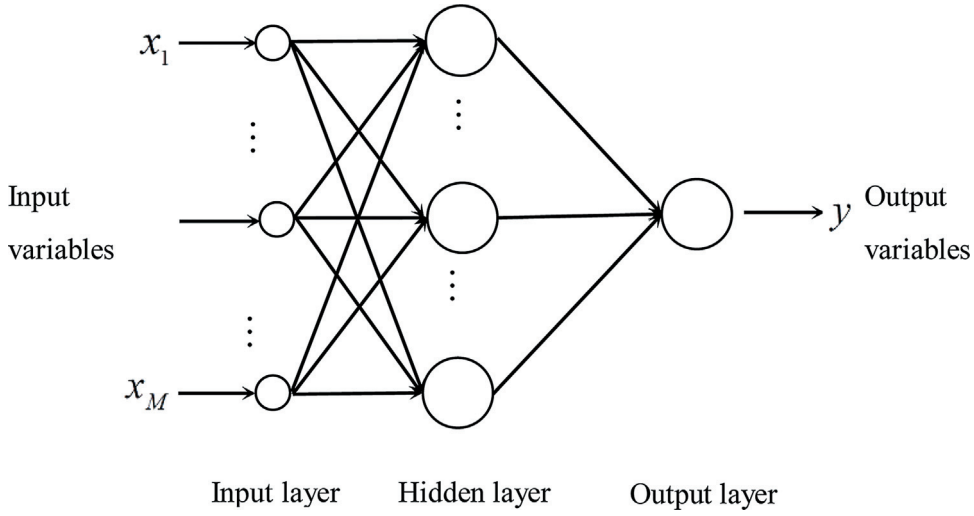

Fig. 1. Topology structure of the 3 layer neural network.

most significant deviation from the real values, y_i. The function is defined as follows (El Amine Ben Seghier et al., 2020):

$$f(x) = \langle w, x \rangle + b \tag{3}$$

where w represents the regression coefficient vector, b represents the bias vector. The function can be formulated as follows (Chou et al., 2017):

$$minimize \frac{1}{2}||w||^2 + C\sum_{i=1}^{n}(\xi_i + \xi_i^*) \tag{4}$$

$$subject to \begin{cases} y_i - \langle w, x_i \rangle - b \le \varepsilon + \xi_i \\ \langle w, x_i \rangle + b - y_i \le \varepsilon + \xi_i^* \\ \xi_i \ge 0, \xi_i^* \ge 0 \end{cases} \tag{5}$$

where ε represents the error, $\xi_i$andξ_i^* are the slack variables. The optimization problem can be further transformed and solved by:

$$f(x) = \sum_{i=1}^{n_{SV}}(\alpha_i - \alpha_i^*)K(x_i, x) \tag{6}$$

where n_{SV} is the number of support vectors, and $K(x_i, x)$ is the kernel function.

RBF was used as the kernel function for its robustness (Hong et al., 2011). K-fold (K = 10) cross-validation technique was applied to select the optimal values of penalty term (C) and the parameters that were involved in the kernel function.

The data used to train and test the ANN model were also used for training and testing of the developed SVM model.

4. Results and analysis

4.1. Correlation of the corrosion rates with the experimental conditions

Pearson's correlation coefficients describing the correlation between corrosion rates and the experimental conditions are shown in Table 1. Correlation analysis between two variables is based on a null hypothesis that there exists a significant correlation between them. It is only when the determined probability value is smaller than 0.05, or in other words, the correlation is significant at the 0.05 level (or 0.01 level), that the hypothesis is accepted (Montgomery and Runger, 2014). As a result, it was found that single DEA, MEA, and PZ has no significant correlation with the corrosion rate. MDEA and total amine both have a negative correlation with the corrosion rate, indicating that generally, the corrosion rate will decrease as the concentrations of MDEA and total amine increase. The solution pH has a significant correlation with the corrosion rate, as shown by a high absolute correlation coefficient, and the negative value indicates that the corrosion rate is lower with higher solution pH. Conductivity of the solutions is positively correlated with the corrosion rate, so when the conductivity is high, a high corrosion rate can also be assumed. Solution type, which consists of rich amine solution and lean amine solution, is strongly correlated with the corrosion rate. Note that the sign (plus or minus) of the correlation coefficient for solution type is meaningless as the virtual variable values for rich and lean amine solution were arbitrarily assigned.

Table 1
Pearson's correlation coefficients between corrosion rate and the environmental conditions.

MDEA concentration	−0.298**
DEA concentration	0.016
MEA concentration	0.045
PZ concentration	0.067
Total amine concentration	−0.238*
pH	−0.467**
Conductivity	0.830**
Solution type	0.818**

* indicates correlation is significant at the 0.05 level (2-tailed).
** indicates correlation is significant at the 0.01 level (2-tailed).

The Pearson's correlation coefficient builds a quantitative relation between corrosion rates and the environmental conditions, however, it contributes little to the understanding of corrosion mechanism in amine solutions. This is because no causal link is guaranteed by the statistical algorithm, and the algorithm is based on a linear association hypothesis, so it is mainly suitable for the assessment of variables that have a linear relationship. In the amine solution system, only conductivity is shown to have a linear relation with the corrosion rate, and this agrees with what is well believed. For solution type, even though the correlation coefficient is significant, this coefficient has no theoretical meaning as the rich solution and the lean solution are not two continuous variables. In addition, rich amine solutions and lean amine solution are different in both CO_2 loading and the other factors, such as pH, concentrations of HSSs, etc., which all affect the corrosion rate in a more complex manner.

It is well accepted that amines are intrinsically not corrosive because of their high pH, and there is no appreciable difference in corrosion rates between different types of amines in the absence of CO_2 (MacNab and Treseder, 1971; LANG and Mason, 1958). However, amines are supposed to contribute to corrosion when CO_2 is involved. Increasing CO_2 loading increases amine solution's corrosivity, hence, rich amine solutions are more corrosive than lean solutions (Kohl and Nielsen, 1997). Riesenfeld and Blohm (1951) believed that the presence of evolved CO_2 from the rich amine solution is the principal cause of corrosion (Riesenfeld and Blohm, 1951), so the oxidising agents driving the corrosion reactions are the same as those commonly present in conventional CO_2-water systems (Nešić, 2007). While this might be a plausiable reason for the relation between solution type and corrosion rate, pH is another important factor, since pH in rich solution is lower than that in lean solution. As a result, Kosseim et al. (1984) suggested that high concentration of protonated amine contributes to corrosion by providing protons for corrosion reaction, and the corrosion mechanism was proposed as (Kosseim et al., 1984):

$$Fe+2RNH_3^+ \rightarrow Fe^{2+} + H_2+2RNH_2 \quad (7)$$

Duan et al. (2013) and Emori et al. (2017) further revised this mechanism and identified the reduction of protonated MDEA as one of the cathodic reactions (Emori et al., 2017; Duan et al., 2013):

$$2MDEAH^+ + 2e^- \rightarrow 2MDEA + H_2 \quad (8)$$

Veawab et al. (1999) proposed that increased concentrations of RNH_3^+ and HCO_3^- in rich solution might dissociate and produce more hydrogen ions via Eqs. (9 and 10) (Veawab et al., 1999), this could account for the decrease of solution pH in CO_2-loaded amine solutions.

$$RNH_3^+ \leftrightarrow H^+ + RNH_2 \quad (9)$$

$$HCO_3^- \leftrightarrow CO_3^{2-} + H^+ \quad (10)$$

In addition, reduction of bicarbonate ion (Eq. 11) and water (Eq. 12), which becomes dominant at a pH range of 6–10, is also the possible cathodic reaction in the amine-CO_2 system (Labiyi, 2016).

$$2HCO_3^- + 2e^- \rightarrow 2CO_3^{2-} + H_2 \quad (11)$$

$$2H_2O + 2e^- \rightarrow 2OH^- + H_2 \quad (12)$$

Apparently, although hydrogen will be evolved in the amine solution, it is difficult to distinguish which reaction dominates the cathodic process.

In CO_2-loaded amine solutions, corrosivity of different amines to carbon steel also varies, this makes the corrosion mechanism more complex. Measurement shows that MDEA has much lower corrosion rates than MEA, DEA and PZ (Labiyi, 2016; Gunasekaran et al., 2013), however, the reason for this is not yet fully understood (Labiyi, 2016). Besides the reactions mentioned above, amount of CO_2 absorbed by the amine solution (Veawab et al., 1999), reactivity of amines to form carbamates (R_3NCOO-) (Veldman, 2000) and/or degradation products in different amines, and formation of $FeCO_3$ scale (Yu et al., 2016; Campbell et al., 2016) are all possible causes. Noting that these causes could occur simultaneously, it is complicated, if not possible, to clearly define the mechanism. According to previous studies, protective scale, i.e., $FeCO_3$, could form in MDEA solutions (Yu et al., 2016). Sedransk Campbell et al. (2016) demonstrated that the $FeCO_3$ layer formed in the case of MDEA provides superior protection from continued corrosion of the carbon steel, and suggested presence of this layer is attributed to the preferred reaction pathway with CO_2 for tertiary amines (Campbell et al., 2016).

For corrosion study in amine solutions, an algorithm which is able to deal with non-linear problem is thus required, and this is why this work is performed. In the development of the ANN-based model, the Pearson's correlation coefficient and significance level shown in Table 1 were further used to determine the major variables affecting the corrosion rates. Currently, five variables, including MDEA concentration, total amine concentration, solution type, pH, and conductivity, were finally determined as major variables. Hence, these five variables were applied as the inputs for the ANN-based model. The effect of five inputs on the ANN model prediction result was studied (by a comparison of the ANN model with eight inputs), and this is discussed in the following section.

4.2. Determination of the best input quantity and number of neurons in the hidden layer

The number of neurons in the hidden layer was initially set as 8, 10, and 12. Moreover, a comparison of the training and testing performance of the ANN models with different input variable quantities (5 and 8) and different hidden layer neuron quantities (8, 10, and 12) was done as shown in Fig. 2. Note that the ANN models herein were named according to their number of neurons in the input, hidden, and output layer. A 5-8-1 type ANN model has five variables in the input layer, eight neurons in the hidden layer, and one output in the output layer. Realizing that the performance of an ANN model varies a lot for each operation (for both training and testing), a total operation of 100 was performed for each type of ANN model. In addition to the best MSE, the MARD, which can be determined as the maximum $\left|(y-\hat{y})/y\right| \times 100\%$ during the training or testing process, was introduced and applied as the index to evaluate the performance of an ANN model in both training and testing processes. A high MARD means there is a large deviation of the predicted value from the actual one and indicates a bad prediction accuracy of the ANN model.

In Fig. 2, the result of ANN models with eight inputs in the input layer is shown in the left column while the result of ANN models for fivewith inputs is shown in the right column. Obviously, ANN models with more inputs in the input layer were associated with a relatively smaller best MSE and a lower MARD in the training process.

A descriptive statistical analysis of the MARD values shown in Fig. 2(a)–(d) was conducted, in which the mean, the standard deviation, square error, minimum and maximum of best MSEs were obtained and tabulated in Table 2, and that of MARDs is shown in Table 3. The result shows the mean, the standard deviation, square error, minimum, and maximum of best MSE values for ANN models with eight inputs were all smaller than those with five inputs. For ANN models with same inputs but varied number of neurons in the hidden layer, values of all the statistical terms increased when the number of neurons in the hidden layer was increased. At the same time, the mean, the standard deviation, square error, minimum, and maximum of MARD values for ANN models with eight inputs were almost all smaller than those with five inputs. For ANN models with same inputs but varied number of neurons in the hidden layer, values of all the statistical terms increased when the number of neurons in the hidden layer was increased. Obviously, the ANN models have better training performance when their number of inputs and number of neurons in the hidden layer are large.

For the testing process, however, a lower MARD was not always seen for the ANN model with more inputs. A descriptive statistical analysis of the MARD values shown in Fig. 2(e) and (f) was conducted, in which the mean, the standard deviation, square error, minimum and maximum of MARDs were obtained and tabulated in Table 4. The analysis shows that except for the minimum MARD values, the mean, the standard deviation, square error, and maximum of MARD values for ANN models with eight inputs were all

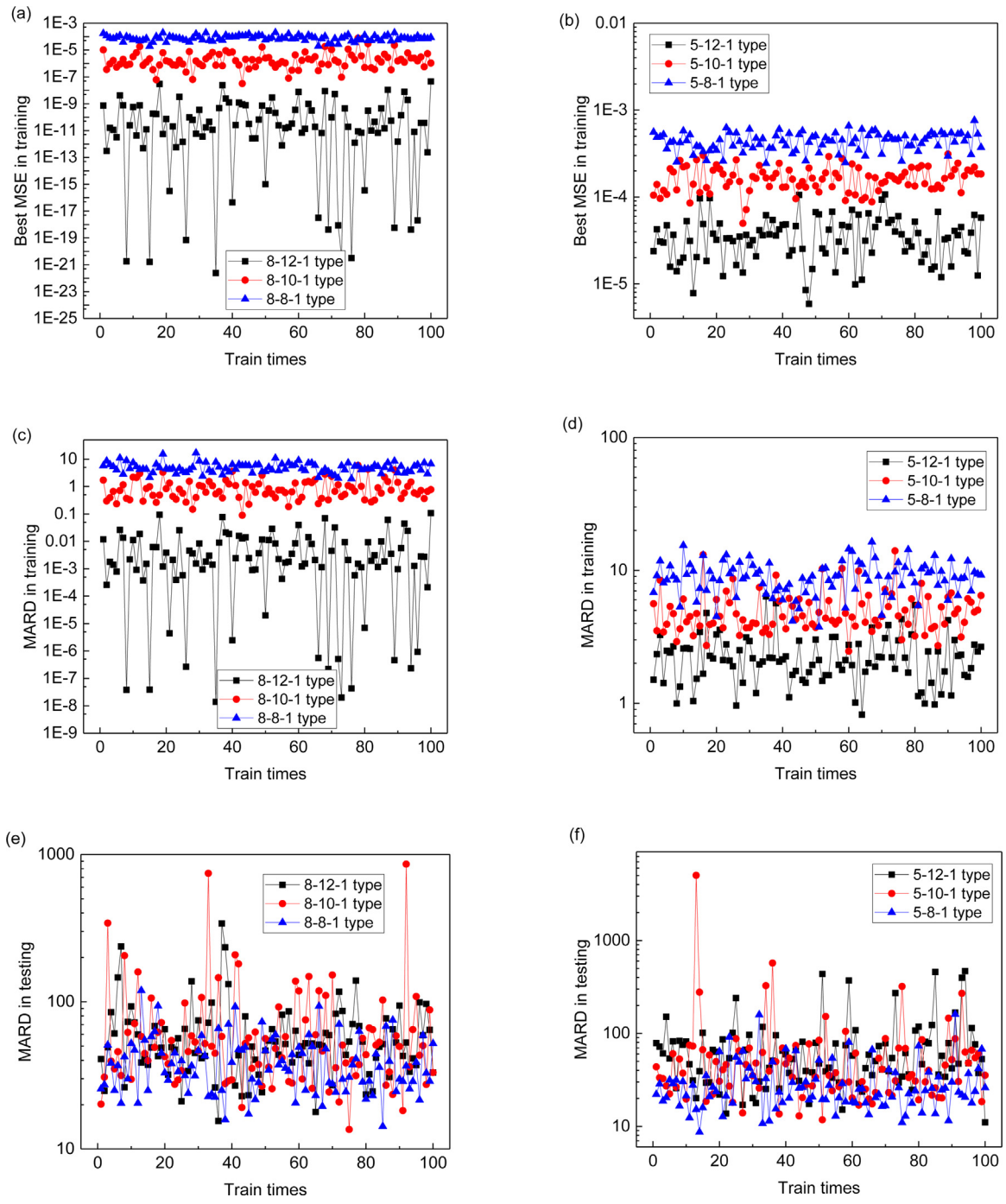

Fig. 2. Best MSE and MARD in training and testing process of different types of ANN models.

Table 2
Statistical description of best MSE in training of the ANN models.

ANN models	Mean	Standard deviation	Square error	Minimum	Maximum
8-12-1 type	1.69E-09	6.15E-09	3.78E-17	2.39E-22	4.62E-08
8-10-1 type	3.96E-06	8.74E-06	7.65E-11	3.21E-08	7.59E-05
8-8-1 type	8.57E-05	3.95E-05	1.56E-09	1.92E-05	0.000199
5-12-1 type	3.76E-05	2.16E-05	4.65E-10	5.9E-06	0.000107
5-10-1 type	0.000167	5.38E-05	2.9E-09	4.97E-05	0.000312
5-8-1 type	0.000443	0.000104	1.09E-08	0.000244	0.000763

smaller than those with five inputs. Where a smaller MARD is preferred for a prediction model, ANN models with five inputs seem to provide predictions of a relatively higher accuracy. More so, the five inputs determined after the correlation analysis are good enough to represent the corrosion rates of the carbon steel in the MDEA-based binary amine mixtures.

Table 3
Statistical description of MARD in training of the ANN models.

ANN models	Mean	Standard deviation	Square error	Minimum	Maximum
8-12-1 type	0.009819	0.019121	0.000366	1.39E-08	0.1078
8-10-1 type	1.039167	0.970628	0.942119	0.08917	5.90289
8-8-1 type	5.265573	2.450803	6.006436	1.92954	16.9013
5-12-1 type	2.294746	1.014208	1.028618	0.82017	6.36646
5-10-1 type	5.087113	2.041921	4.16944	2.46447	14.0131
5-8-1 type	9.032124	2.530737	6.404628	3.75073	16.4027

Table 4
Statistical description of MARD in testing of the ANN models.

ANN models	Mean	Standard deviation	Square error	Minimum	Maximum
8-12-1 type	62.29781	46.36791	2149.983	15.4941	339.936
8-10-1 type	76.87512	115.4212	13322.04	13.571	860.101
8-8-1 type	41.77564	23.53282	553.7938	14.2616	183.281
5-12-1 type	79.44392	90.24047	8143.342	11.0541	468.525
5-10-1 type	109.1978	501.9114	251915	11.7571	5019.93
5-8-1 type	33.22111	28.86544	833.2135	8.66467	183.281

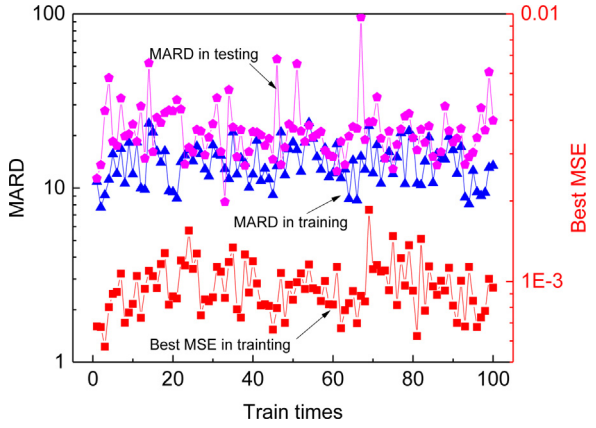

Fig. 3. Best MSE and MARD for calculation with 5-6-1 type ANN model.

As shown in Fig. 2, ANN models with different number of neurons in the hidden layer have different best MSEs and MARDs in the training process, as well as different MARDs in the testing process. Similar to the effect of the number of inputs on the best MSE and MARD in the training process, ANN models with more neurons in the hidden layer had better performance, in other words, compared to ANN models that had either five or eight inputs, models with 12 neurons in the hidden layer had the lowest best MSE and smallest MARD in the training process. However, when it comes to MARD in the testing process, ANN models with least neuron numbers, e.g., eight, in the hidden layer, had the smallest MARD value. ANN models with ten neurons in the hidden layer were an exception, their MARDs in the testing process were always higher than those with 12 neurons; it seems that an ANN model with less number of neurons in the hidden layer has better performance in the testing process. This was further proven to be true when the MARD in the testing process of a 5-6-1 type ANN model had a minimum MARD value of 8.32, during a total operation time of 100, as shown in Fig. 3.

While the decrease in number of neurons in the hidden layer of an ANN model reduces the MARD value in the testing process and enhances the performance of an ANN model in prediction, the MARD value in the training process, however, increased. It can be found in Fig. 3 that for the 5-6-1 type ANN model, the MARD level in training process had increased and approached that of the testing process. It is believed that there is a paradox between the performance of an ANN model in the training process and that in the testing process, and this paradox could be attributable to the fact that the data used in the testing process represents some new scenarios that are not covered by the data used in the training process. Thus, a compromise has to be made to maintain a good performance in the training process. For a good prediction ability, the number of neurons in the hidden layer of the developed ANN model was determined to be eight.

Table 5
Performance in training and testing of the SVM models.

SVM models	Training		Testing
	MSE	MARD	MARD
8 variables	0.0014938	25.0208	24.259
5 variables	0.0015369	20.0631	38.4144

4.3. Comparison of the ANN models with the SVM models

The cross plot of the developed SVM models with eight or five input variables for testing and training data points is shown in Fig. 4. It shows that most of the predicted value matches well with the experimental value for both models. However, significant deviation exists for some data points in training and testing. Significant MARD in training is found for the SVM model with eight inputs, and significant MARD in testing is found for the SVM model with five inputs.

A statistical description of the SVM models in training and testing is shown in Table 5. It can be found the number of variables also affect the performance of the developed SVM model. For the SVM model with eight variables, its MSE and MARD are both smaller than that of the model with five variables; however, its MARD is relatively larger.

A comparison of the performance of the SVM models with the ANN models can be made. Apparently, for training process, the ANN models had better performance both in MSE and MARD. For testing, ANN models had better minimum MARD than that of the SVM models. It can be concluded that the developed ANN models have a better performance as compared to the SVM models.

4.4. ANN model development for pH and conductivity prediction

Given that pH and conductivity of the MDEA-based binary amine solutionmixtures were not always available as input for the developed 5-8-1 type ANN model, ANN models for pH and conductivity prediction were developed. The experimental database created for the corrosion rate prediction ANN model was also used in the development of ANN models for pH and conductivity. The ANN model for

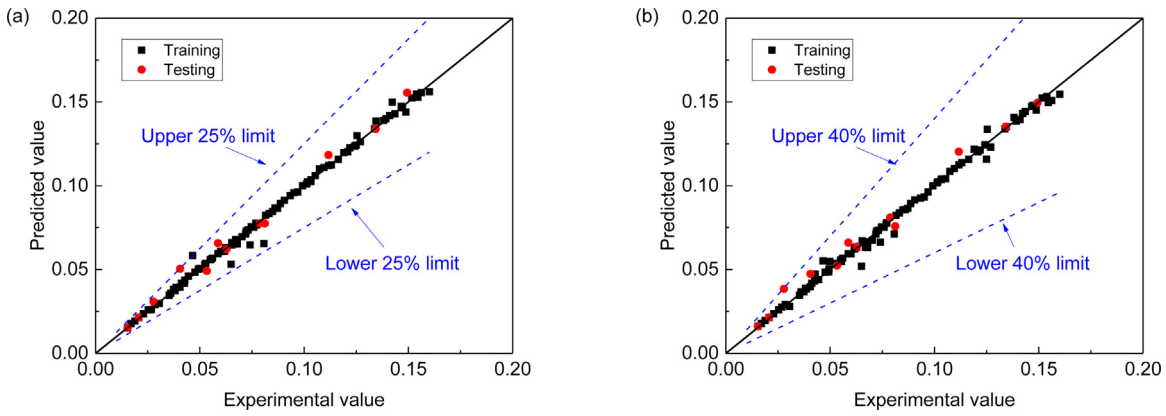

Fig. 4. Cross plot of the predicted corrosion rate with the developed SVM model vs. experimental result: (a) SVM model with eight input variables, (b) SVM model with five input variables.

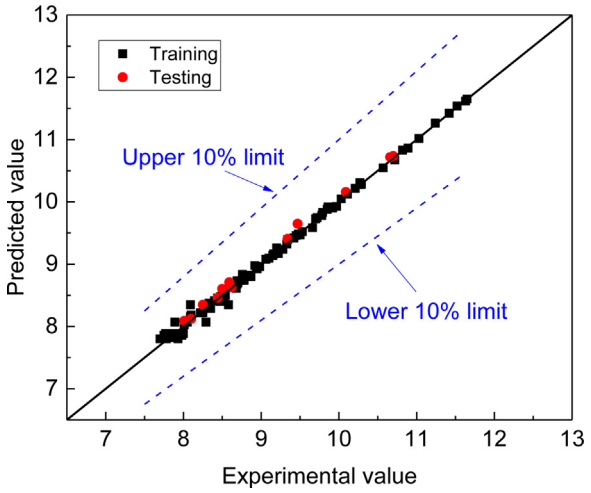

Fig. 5. Cross plot of the predicted pH with the developed ANN model vs. experimental result.

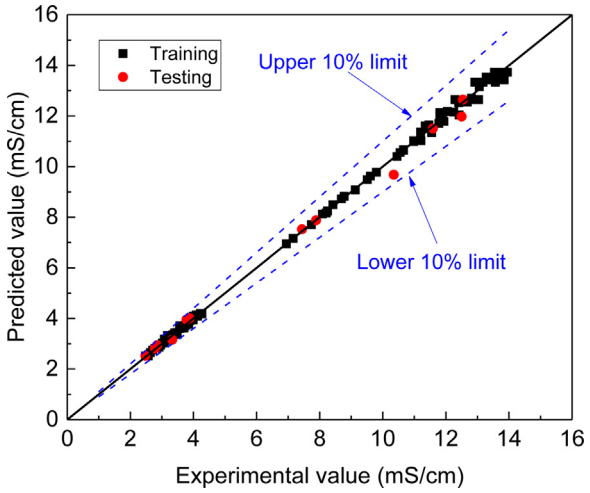

Fig. 6. Cross plot of the predicted conductivity with the developed ANN model vs. experimental result.

pH and conductivity prediction employed the same algorithm and functions as those for the development of the ANN model for corrosion rate prediction. The difference was that five variables used as inputs: MDEA concentration, DEA concentration, MEA concentration, PZ concentration, and solution type. The number of neurons in the hidden layer for both ANN models was arbitrarily determined to be eight, while the output layer has one neuron for pH and conductivity, respectively.

The ANN model developed for pH prediction was trained and tested by comparing the predicted pH value with the experimental value, as shown in Fig. 5. It shows that the predicted data, both training, and testing, was located well adjacent to the iso-line within the ±10 % limit range. The largest MARD in the testing process was determined to be 1.88.

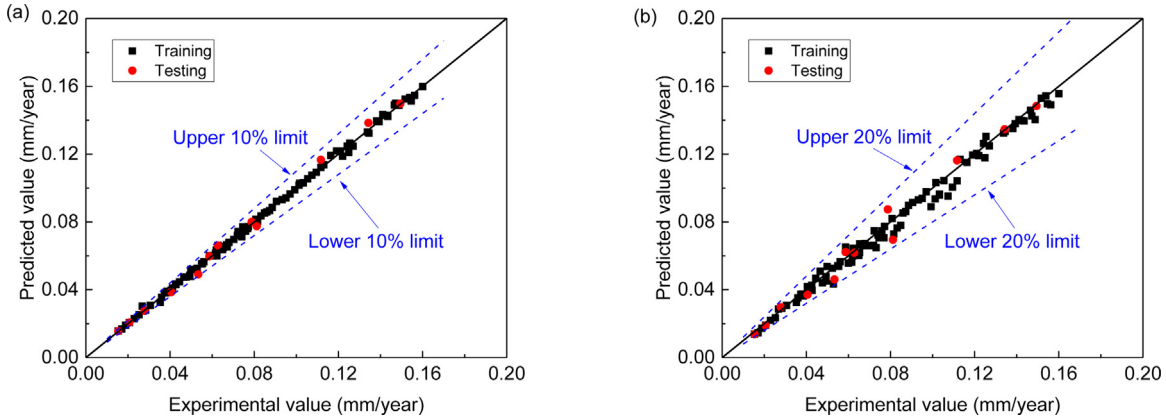

Fig. 7. Cross plot of the prediction result of corrosion rate with the developed ANN model vs. experimental result: (a) for prediction with experimental pH and conductivity, (b) for prediction with predicted pH and conductivity in testing process.

The ANN model for conductivity prediction was also trained and tested, and the performance of the model is shown in Fig. 6. The developed ANN model also had a good accuracy in conductivity prediction. The MARD in the testing process of the developed ANN model is 6.50, which is a bit larger than that of the pH prediction.

4.5. Performance of the developed ANN model in corrosion rate prediction

The developed 5-8-1 type ANN model for corrosion rate prediction of carbon steel in the MDEA-based binary amines mixtures was further trained and tested. When the data from the experimental database was used for the training and testing, the predicted corrosion rates were validated and found to have good matching with the experimental data, as shown in Fig. 7(a), all the data points fell well within the ±10 % limit range. The MARD in the testing process was determined to be 7.97. However, when the predicted pH and conductivity were included in the testing database, instead of the experimental ones, the prediction results were found to fluctuate stronger from the iso-line, as shown in Fig. 7(b). The MARD in the testing process was found to be 14.46. Trials were made by also including the predicted pH and conductivity in the training database, and a larger MARD, i.e., 15.05, in the testing process was obtained. Therefore, to have a good performance in predicting corrosion rate with the developed 5-8-1 type ANN model, the experimentally determined pH and conductivity for the amine solutions would be the first choice of input variables.

5. Conclusions

In this study, an ANN model for the corrosion prediction of carbon steel in MDEA-based binary amine mixtures with MEA, DEA, or PZ at various concentrations was developed. Experimental studies were performed to obtain the corrosion rate data of Q345R steel over multiple conditions by the weight-loss method, and the data was used to train and test the developed ANN model and SVM model. The ANN model employed a BP MLP network that has three layers: the input layer has five input variables, the hidden layer has a neuron quantity of eight, and the output layer has one output variable, i.e., corrosion rate. The correlation analysis method proved helpful in the determination of input variables, which include MDEA concentration, total amine concentration, pH, conductivity, and solution type. Increasing the neuron quantity in the hidden layer would enhance the training accuracy; however, it reduces the testing accuracy. In the development of the SVM models, RBF is used as the kernel function, and K-fold cross-validation technique is applied to select the optimal model values. The number of input variables is found to affect the performance of the developed SVM model. The SVM model with eight variables has better training and testing performance than that of the model with five variables. A new index, MARD, was suggested to quantify the performance of the ANN model. The MARD in prediction of the developed ANN model was determined to be 8.66 % when the values of the five input variables are all experimentally determined. A comparison of performance in both training and testing showed that the ANN model outperforms the SVM model.

For cases where amine solution pH and conductivity are not available, they could be obtained with the ANN model developed for pH and conductivity prediction, respectively. However, when the predicted pH and conductivity were substituted into the ANN model for corrosion rate prediction, the prediction accuracy would become worse.

Declaration of Competing Interest

The authors report no declarations of interest.

Acknowledgments

This work was supported by the Key Special Project of the National Key Research & Development Plan during the 13th Five-Year Period P̈ublic Safety Risk Control and Emergency Technology Equipment(̈2016YFC0802302), the Natural Science Foundation of Shandong Province (Project No.: ZR2019BEE040), the Fundamental Research Funds for the Central Universities (Project No.: 18CX02001A)

Appendix A. Matrix of the experimental conditions and results

No.	Type	Concentration %					pH	Conductivity mS cm^{-1}	Temperature °C	Corrosion rate mm/year
		MDEA	DEA	MEA	PZ	Total amine				
1	Lean	25	0	0	0	25	8.44	2.48	80	0.01541
2	Lean	20	5	0	0	25	8.54	2.71	80	0.02296
3	Lean	15	10	0	0	25	8.59	2.85	80	0.02785
4	Lean	30	0	0	0	30	8.46	2.57	80	0.01706
5	Lean	25	5	0	0	30	8.7	2.91	80	0.03056
6	Lean	20	10	0	0	30	8.77	3.08	80	0.03603
7	Lean	35	0	0	0	35	8.5	2.64	80	0.01886
8	Lean	30	5	0	0	35	8.86	3.02	80	0.03863
9	Lean	25	10	0	0	35	8.98	3.13	80	0.04767
10	Lean	20	15	0	0	35	9.2	3.28	80	0.05543
11	Lean	40	0	0	0	40	8.62	2.78	80	0.02072
12	Lean	35	5	0	0	40	9.15	3.2	80	0.04942
13	Lean	30	10	0	0	40	9.34	3.42	80	0.06196
14	Lean	25	15	0	0	40	9.66	3.49	80	0.06797
15	Lean	45	0	0	0	45	8.83	2.96	80	0.02529
16	Lean	40	5	0	0	45	9.45	3.34	80	0.06504
17	Lean	35	10	0	0	45	9.78	3.56	80	0.05867
18	Lean	30	15	0	0	45	10.03	3.64	80	0.0524
19	Lean	25	20	0	0	45	10.29	3.81	80	0.04118
20	Lean	25	0	0	0	25	8.44	2.48	80	0.01541
21	Lean	20	0	5	0	25	9.06	3.74	80	0.04283
22	Lean	15	0	10	0	25	9.53	3.16	80	0.07025
23	Lean	30	0	0	0	30	8.46	2.57	80	0.01706
24	Lean	25	0	5	0	30	9.22	3.08	80	0.05288
25	Lean	20	0	10	0	30	9.47	3.33	80	0.05875

26	Lean	35	0	0	0	35	8.5	2.64	80	0.01886
27	Lean	30	0	5	0	35	9.48	3.23	80	0.06277
28	Lean	25	0	10	0	35	9.79	3.41	80	0.07408
29	Lean	20	0	15	0	35	10.21	3.64	80	0.04987
30	Lean	40	0	0	0	40	8.62	2.78	80	0.02072
31	Lean	35	0	5	0	40	9.97	3.49	80	0.06692
32	Lean	30	0	10	0	40	10.27	3.76	80	0.04658
33	Lean	25	0	15	0	40	10.72	3.87	80	0.03819
34	Lean	45	0	0	0	45	8.83	2.96	80	0.02529
35	Lean	40	0	5	0	45	10.11	3.57	80	0.05606
36	Lean	35	0	10	0	45	10.66	3.88	80	0.04056
37	Lean	30	0	15	0	45	11.03	4	80	0.03532
38	Lean	25	0	20	0	45	11.52	4.27	80	0.02681
39	Lean	25	0	0	0	25	8.44	2.48	80	0.01541
40	Lean	20	0	0	5	25	9.33	3.85	80	0.06
41	Lean	15	0	0	10	25	9.92	3.29	80	0.07227
42	Lean	30	0	0	0	30	8.46	2.57	80	0.01706
43	Lean	25	0	0	5	30	9.5	3.18	80	0.06717
44	Lean	20	0	0	10	30	9.85	3.46	80	0.07588
45	Lean	35	0	0	0	35	8.5	2.64	80	0.01886
46	Lean	30	0	0	5	35	9.86	3.36	80	0.08077
47	Lean	25	0	0	10	35	10.28	3.58	80	0.06228
48	Lean	20	0	0	15	35	10.82	3.86	80	0.04937
49	Lean	40	0	0	0	40	8.62	2.78	80	0.02072
50	Lean	35	0	0	5	40	10.57	3.7	80	0.055
51	Lean	30	0	0	10	40	10.89	3.99	80	0.04453
52	Lean	25	0	0	15	40	11.42	4.13	80	0.04049
53	Lean	45	0	0	0	45	8.83	2.96	80	0.02529
54	Lean	40	0	0	5	45	10.7	3.78	80	0.05335
55	Lean	35	0	0	10	45	11.24	4.09	80	0.04262
56	Lean	30	0	0	15	45	11.63	4.22	80	0.03741
57	Lean	25	0	0	20	45	11.65	2.96	80	0.02843
58	Rich	25	0	0	0	25	7.7	13.54	80	0.1074
59	Rich	20	5	0	0	25	7.78	12.68	80	0.1472
60	Rich	15	10	0	0	25	7.85	12.25	80	0.14353
61	Rich	30	0	0	0	30	7.75	13.28	80	0.09927
62	Rich	25	5	0	0	30	7.94	11.81	80	0.14879
63	Rich	20	10	0	0	30	8.01	11.35	80	0.13816
64	Rich	35	0	0	0	35	7.77	13.44	80	0.08157
65	Rich	30	5	0	0	35	8.1	11.59	80	0.13434
66	Rich	25	10	0	0	35	8.22	11.21	80	0.12536
67	Rich	20	15	0	0	35	8.4	10.55	80	0.11643
68	Rich	40	0	0	0	40	7.89	12.92	80	0.07317
69	Rich	35	5	0	0	40	8.35	10.98	80	0.12095
70	Rich	30	10	0	0	40	8.5	10.35	80	0.1117
71	Rich	25	15	0	0	40	8.78	8.69	80	0.1033
72	Rich	45	0	0	0	45	8.09	12.29	80	0.06159
73	Rich	40	5	0	0	45	8.69	9.51	80	0.09055
74	Rich	35	10	0	0	45	8.92	8.09	80	0.08603
75	Rich	30	15	0	0	45	9.16	7.74	80	0.07721
76	Rich	25	20	0	0	45	9.42	6.95	80	0.06536
77	Rich	25	0	0	0	25	7.78	13.68	80	0.10954
78	Rich	20	0	5	0	25	7.86	12.81	80	0.15623
79	Rich	15	0	10	0	25	8.01	12.5	80	0.14943
80	Rich	30	0	0	0	30	7.83	13.41	80	0.10125
81	Rich	25	0	5	0	30	8.1	12.05	80	0.15458
82	Rich	20	0	10	0	30	8.09	11.46	80	0.14231
83	Rich	35	0	0	0	35	7.85	13.57	80	0.0832
84	Rich	30	0	5	0	35	8.34	11.94	80	0.14105
85	Rich	25	0	10	0	35	8.47	11.55	80	0.1345
86	Rich	20	0	15	0	35	8.48	10.66	80	0.12493
87	Rich	40	0	0	0	40	8.05	13.18	80	0.07464
88	Rich	35	0	5	0	40	8.52	11.2	80	0.12699
89	Rich	30	0	10	0	40	8.59	10.45	80	0.12196
90	Rich	25	0	15	0	40	8.87	8.78	80	0.10537
91	Rich	45	0	0	0	45	8.25	12.54	80	0.06282
92	Rich	40	0	5	0	45	8.78	9.61	80	0.09508
93	Rich	35	0	10	0	45	9.1	8.25	80	0.08861
94	Rich	30	0	15	0	45	9.34	7.89	80	0.07876
95	Rich	25	0	20	0	45	9.7	7.16	80	0.07195
96	Rich	25	0	0	0	25	7.93	13.95	80	0.11173
97	Rich	20	0	0	5	25	8.01	13.06	80	0.16006
98	Rich	15	0	0	10	25	8.25	12.87	80	0.15391
99	Rich	30	0	0	0	30	7.98	13.68	80	0.10328
100	Rich	25	0	0	5	30	8.34	12.41	80	0.15166
101	Rich	20	0	0	10	30	8.33	11.81	80	0.14658
102	Rich	35	0	0	0	35	8	13.85	80	0.08487
103	Rich	30	0	0	5	35	8.68	12.42	80	0.13928

104	Rich	25	0	0	10	35	8.64	11.78	80	0.13381
105	Rich	20	0	0	15	35	8.74	10.98	80	0.11308
106	Rich	40	0	0	0	40	8.29	13.57	80	0.07688
107	Rich	35	0	0	5	40	8.69	11.42	80	0.12424
108	Rich	30	0	0	10	40	8.76	10.66	80	0.11909
109	Rich	25	0	0	15	40	9.22	9.13	80	0.1016
110	Rich	45	0	0	0	45	8.58	13.04	80	0.06533
111	Rich	40	0	0	5	45	8.95	9.8	80	0.09698
112	Rich	35	0	0	10	45	9.28	8.42	80	0.09331
113	Rich	30	0	0	15	45	9.72	8.21	80	0.08726
114	Rich	25	0	0	20	45	10.09	7.44	80	0.0812

References

Abiodun, O.I., Jantan, A., Omolara, A.E., Dada, K.V., Mohamed, N.A., Arshad, H., 2018. State-of-the-art in artificial neural network applications: a survey. Heliyon 4, e00938.

Ahlgren, P., Jarneving, B., Rousseau, R., 2003. Requirements for a cocitation similarity measure, with special reference to Pearson's correlation coefficient. J. Am. Soc. Inf. Sci. Technol. 54, 550–560.

Beale, M.H., Hagan, M.T., Demuth, H.B., 2016b. In: MathWorks (Ed.), Neural Network Toolbox: for Use with MATLAB: User's Guide: Version 2016b.

Campbell, K.L.S., Zhao, Y., Hall, J.J., Williams, D.R., 2016. The effect of CO_2-loaded amine solvents on the corrosion of a carbon steel stripper. Int. J. Greenh. Gas Control. 47, 376–385.

Chen, J., Guo, Q., Hua, Y., Tang, J., Fu, H., 2014. An experimental study of absorption and desorption of blended amine solutions MDEA+MEA/DEA for natural gas decarburization (In Chinese). Nat. Gas Ind. B 34, 137–143.

Choi, Y.-S., Nešić, S., Duan, D., Jiang, S., 2012. Mechanistic modeling of carbon steel corrosion in a MDEA-based CO_2 capture process. Corrosion 2012.

Chou, J.-S., Ngo, N.-T., Chong, W.K., 2017. The use of artificial intelligence combiners for modeling steel pitting risk and corrosion rate. Eng. Appl. Artif. Intell. 65, 471–483.

Colorado-Garrido, D., Ortega-Toledo, D.M., Hernández, J.A., González-Rodríguez, J.G., Uruchurtu, J., 2008. Neural networks for Nyquist plots prediction during corrosion inhibition of a pipeline steel. J. Solid State Electrochem. 13, 1715–1722.

Duan, D., Choi, Y.-S., Jiang, S., Nešić, S., 2013. Corrosion mechanism of carbon steel in MDEA-based CO_2 capture plants. In: Corrosion 2013. NACE International.

El Amine Ben Seghier, M., Keshtegar, B., Tee, K.F., Zayed, T., Abbassi, R., Trung, N.T., 2020. Prediction of maximum pitting corrosion depth in oil and gas pipelines. Eng. Fail. Anal. 112.

Emori, W., Jiang, S.L., Duan, D.L., Ekerenam, O.O., Zheng, Y.G., Okafor, P.C., Qiao, Y.X., 2017. Corrosion behavior of carbon steel in amine-based CO_2 capture system: effect of sodium sulfate and sodium sulfite contaminants. Mater. Corros. 68, 674–682.

Eustaquio-Rincón, R., Rebolledo-Libreros, M.E., Trejo, A., Molnar, R., 2008. Corrosion in aqueous solution of two alkanolamines with CO_2 and H_2S: N-Methyldiethanolamine + Diethanolamine at 393 K. Ind. Eng. Chem. Res. 47, 4726–4735.

Fang, L., 2004. Determination of heat stable salts amine by solid-phase extraction coupled with ion chromatography (In Chinese). J. Instrum. Anal. 23, 84–87.

G1-03, A., 2011. Standard Practice for Preparing, Cleaning, and Evaluating Corrosion Test Specimens. ASTM International, West Conshohocken.

Ghiasi, M.M., Bahadori, A., Zendehboudi, S., 2014. Estimation of the water content of natural gas dried by solid calcium chloride dehydrator units. Fuel 117, 33–42.

Gunasekaran, P., 2012. Corrosion Evaluation for Absorption-Based CO_2 Capture Process Using Single and Blended Amines. Faculty of Graduate Studies and Research, University of Regina.

Gunasekaran, P., Veawab, A., Aroonwilas, A., 2013. Corrosivity of single and blended amines in CO_2 capture process. Energy Procedia 37, 2094–2099.

Hong, W.-C., Dong, Y., Chen, L.-Y., Wei, S.-Y., 2011. SVR with hybrid chaotic genetic algorithms for tourism demand forecasting. Appl. Soft Comput. 11, 1881–1890.

Hu, Q., Liu, Y., Zhang, T., Geng, S., Wang, F., 2019. Modeling the corrosion behavior of Ni-Cr-Mo-V high strength steel in the simulated deep sea environments using design of experiment and artificial neural network. J. Mater. Sci. Technol. 35, 168–175.

Kohl, A.L., Nielsen, R., 1997. Gas Purification. Gulf Publishing Company, Houston, Texas.

Kosseim, A., McCullough, J., Butwell, K., 1984. Corrosion-inhibited amine guard ST process. Chem. Eng. Prog. 80, 64–71.

Labiyi, F., 2016. Electrochemical Kinetics and Mechanisms of Iron Oxidation in CO_2-containing Aqueous Monoethanolamine. Imperial College London.

LANG, F.S., Mason Jr, J., 1958. Corrosion in amine gas treating solutions. Corrosion 14, 65–68.

Li, J., Yan, D., Zhao, H., 2005. An momentum BP neural network algorithm and application (In Chinese). Electrotechnical Application 24, 42–44.

MacNab, A., Treseder, R., 1971. Materials requirements for a gas treating process. Mater. Perform. 10, 21–26.

Montgomery, D.C., Runger, G.C., 2014. Applied Statistics and Probability for Engineers, 6th edition. John Wiley & Sons, Hoboken.

Nainar, M., Veawab, A., 2009. Corrosion in CO_2 capture process using blended monoethanolamine and piperazine. Ind. Eng. Chem. Res. 48, 9299–9306.

Nešić, S., 2007. Key issues related to modelling of internal corrosion of oil and gas pipelines – a review. Corros. Sci. 49, 4308–4338.

Nielsen, R.B., Lewis, K.R., McCullough, J.G., Hansen, D.A., 1995. Corrosion in refinery amine systems. In: Corrosion 95. NACE International, Orlando.

Rennie, S., 2006. Corrosion and Materials Selection for Amine Service. Materials Forum, Citeseer, pp. 126–130.

Riesenfeld, F., Blohm, C., 1951. Corrosion resistance of alloys in amine gas treating systems. Pet. Refin. 30, 107–115.

Rocabruno-Valdés, C.I., González-Rodriguez, J.G., Díaz-Blanco, Y., Juantorena, A.U., Muñoz-Ledo, J.A., El-Hamzaoui, Y., Hernández, J.A., 2019. Corrosion rate prediction for metals in biodiesel using artificial neural networks. Renew. Energy 140, 592–601.

Saghafi, H., Arabloo, M., 2017. Modeling of CO_2 solubility in MEA, DEA, TEA, and MDEA aqueous solutions using AdaBoost-Decision Tree and Artificial Neural Network. Int. J. Greenh. Gas Control. 58, 256–265.

Tanthapanichakoon, W., Veawab, A., 2005. Polarization behavior and performance of inorganic corrosion inhibitors in monoethanolamine solution containing carbon dioxide and heat-stable salts. Corrosion 61, 371–380.

Veawab, A., Tontiwachwuthikul, P., Chakma, A., 1999. Corrosion behavior of carbon steel in the CO_2 absorption process using aqueous amine solutions. Ind. Eng. Chem. Res. 38, 3917–3924.

Veldman, R., 2000. Alkanolamine solution corrosion mechanisms and inhibition from heat stable salts and CO_2. In: Corrosion 2000. NACE International.

Xu, Y., Jin, R., 2018. Measurement of reinforcement corrosion in concrete adopting ultrasonic tests and artificial neural network. Constr. Build. Mater. 177, 125–133.

Yu, L.C.Y., Sedransk Campbell, K.L., Williams, D.R., 2016. Carbon steel corrosion in piperazine-promoted blends under CO_2 capture conditions. Int. J. Greenh. Gas Control. 55, 144–152.

Zhang, G., 2017. Studies on Foaming Characteristics of Decarburization Amine Solution of Natural Gas. China University of Petroleum (East China).

Zheng, L.F., Landon, J., Zou, W.C., Liu, K.L., 2014. Corrosion benefits of piperazine as an alternative CO_2 capture solvent. Ind. Eng. Chem. Res. 53, 11740–11746.